

# Faster and more diverse de novo molecular optimization with double-loop reinforcement learning using augmented SMILES

Esben Jannik Bjerrum\*<sup>1</sup>, Christian Margreitter<sup>1</sup>, Thomas Blaschke<sup>1</sup>, Raquel Lopez-Rios de Castro<sup>1,2</sup>

1) Odyssey Therapeutics, Cambridge, MA, USA

2) Department of Physics and Department of Chemistry, King's College, London, UK

\*) [esben@odysseytx.com](mailto:esben@odysseytx.com)

Molecular generation via deep learning models in combination with reinforcement learning is a powerful way of generating proposed molecules with desirable properties. By defining a multi-objective scoring function, it is possible to generate thousands of ideas for molecules that scores well, which makes the approach interesting for drug discovery or material science purposes. However, if the scoring function is expensive regarding resources, such as time or computation, the high number of function evaluations needed for feedback in the reinforcement learning loop becomes a bottleneck. Here we propose to use double-loop reinforcement learning with simplified molecular line entry system (SMILES) augmentation to use scoring calculations more efficiently and arrive at well scoring molecules faster. By adding an inner loop where the SMILES strings generated are augmented to alternative non-canonical SMILES and used for additional rounds of reinforcement learning, we can effectively reuse the scoring calculations that are done on the molecular level. This approach speeds up the learning process regarding scoring function calls, as well as it protects moderately against mode collapse. We find that augmentation repeats between 5-10x seem safe for most scoring functions and additionally increase the diversity of the generated compounds, as well as making the sampling runs of chemical space more reproducible

## Introduction

Molecular generation via deep learning architectures such as recurrent neural networks trained on simplified molecular line entry system (SMILES) strings appeared some five years[1]–[3] ago as a way to generate molecules that closely resemble the training set used with regard to molecular properties. SMILES strings has also been used together with GANs[4] and variational autoencoders[5] for generative purposes.

The SMILES-LSTM based generation algorithms were quickly coupled to optimization algorithms, where early attempts used transfer learning and fine-tuning[3], other solutions using reinforcement learning soon appeared[2]. Using reinforcement learning allowed for flexible definition of compound scoring functions that could take multiple desirable properties into account simultaneously, which may not depend on having a suitable dataset size of known ligands at all. The original Reinvent[2] was further developed and new versions were released[6], as well as variants for link-design[7] and

library design[8] were developed. The large array of de novo molecular generative algorithms, including SMILES based ones, has been reviewed previously[9]–[11]

A drawback of the reinforcement learning is that it may require a lot of scoring function evaluations to optimize the agent into a productive state. In the first REINVENT paper, 384,000 scoring function evaluations were used to optimize the agent. This is not an issue if the scoring function has a trivial computational demand, such as by simple scores such as QED, cLogP or fast QSAR models, but do get increasingly problematic if more time- or resource consuming methods such as automated molecular docking and scoring, quantum chemical calculations or free energy estimation methods are used for the scoring function. This problem was addressed recently by Thomas and co-workers, who proposed to use what they call augmented hill climb reinforcement learning.[12] However, it is important to note that they are not using SMILES augmentation[13], [14] as the name could imply, neither are they using a standard hill-climb algorithm[15], [16] which are iterative fine-tuning on the best scoring compounds sampled. In practice they do reinforcement learning on the 50% best scoring compounds of the generated SMILES of the batch. By doing this they demonstrate the speed up of the reinforcement learning, but unfortunately does not look extensively at the diversity of the compounds. Gao and Fu and co-workers recently approached the issue of efficiency by setting up a benchmark with several metrics and testing multiple generative algorithms.[17] ReInvent 2.0 came out as a solid contender, but only after tuning the sigma parameter, which controls how much the scoring function is allowed to influence the loss which puts less emphasis on the loglikelihood of the prior. However, the tuning of sigma to larger values puts less emphasis on the prior and may therefore likely increases the risk of over-exploitation which could lead to lower diversity and unrealistic molecules, an issue the benchmark does not address and which the authors acknowledge as a drawback to work on in the future.[18]

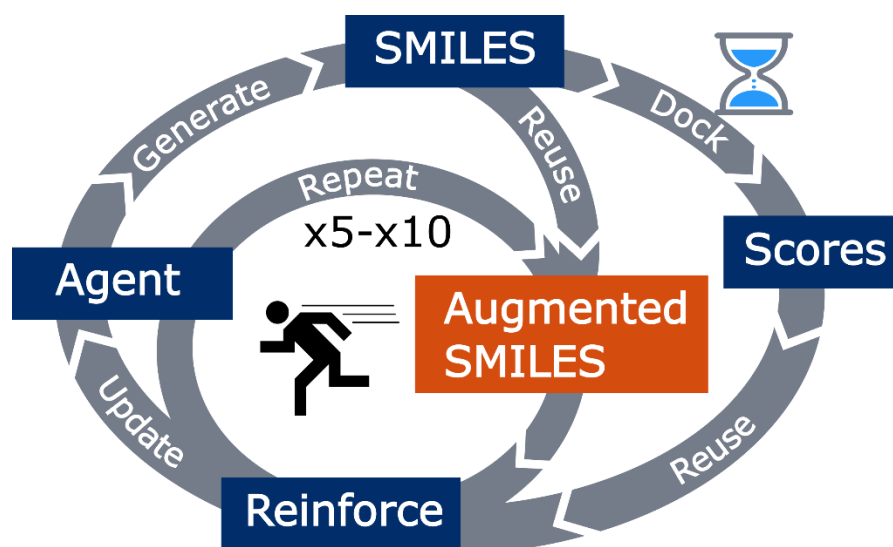


*Figure 1:* The Augmented double loop reinforcement learning. By reusing the scores for the molecules and producing augmented SMILES strings that are dissimilar to the ones generated by the agent, it is possible to update the agent several times before new SMILES strings need to be sampled, parsed to molecules, and scored.

Here we present a method to speed up reinforcement learning optimizations without changing the sigma parameter, but instead use SMILES augmentation for more efficient feedback to the agent and faster learning. SMILES augmentation, also called SMILES enumeration[13] or SMILES randomization[14], is the process of using several different non-canonical SMILES of the same molecule for improved deep learning. It has shown improvements to many deep learning algorithms, within deep learning QSAR[13], molecular generation[14], [19], latent space optimization[20], unsupervised pretraining[21] and retrosynthesis prediction[22]. By combining it with the

reinforcement learning, we both increase the efficiency as well as it increases molecular diversity and reproducibility of the molecular optimization.

## Methods

ReInvent 2.0[6] was forked and reprogrammed so that reinforcement learning loop had an inner loop that reuses the scores molecules (obtained from agent generated SMILES) in the outer loop. In the inner loop alternative SMILES sequences are created via SMILES augmentation[13] and used to further reinforce the agent with the already obtained scores for that molecule (Figure 1). The number of augmentations done in the inner loop is a new configurable hyper-parameter. The number of updates of the agent via reinforcement learning is thus decoupled from slow scoring components, such as docking. As the generation of augmented SMILES and backpropagation in the reinforcement learning is much faster than the scoring function components, the overall process can run much faster and with less scoring function evaluations. We named the updated ReInvent, Diania.

### Similarity task

The first task tested was entirely exploitative, as the task is to optimize a fingerprint based Tanimoto similarity to a target compound. The target compound was chosen to be Aripiprazole from the GuacaMol benchmark[16] (SMILES: "Clc4cccc(N3CCN(CCCCOc2ccc1c(NC(=O)CC1)c2)CC3)c4Cl"). The similarity scoring component of Diania was configured with the target SMILES and given a weight of one. Experience replay was used with a memory size of 100 and a sample size of 10. No diversity filter was employed[23]. Batch size for generation was 64, and learning rate was default 0.0001 unless otherwise noted. Sigma was kept at the default, 128, for all runs. The prior was the random.prior.new obtained from the Reinvent Community repository[24].

Two series of experiments were made scanning the augmentation and learning rate hyperparameters, respectively. The number of augmentations was varied in the range [1, 2, 5, 10, 20, 50, 100, 200] with the learning rate fixed at default (0.0001), and in the other experiment, the augmentation was fixed at one, and the learning rate was varied by multiplying the default with [1, 2, 5, 10, 20, 40, 60, 80, 100, 200], so the resulting learning rate was varied between 0.0001 and 0.02. Finally, a grid search was set up, where both the number of augmentations and learning rate were varied as [1, 2, 3, 5, 10, 20] and [1, 2, 3, 5, 7, 15], respectively. 1000 steps were used for the runs, corresponding to roughly 64,000 scoring function evaluations. All experiments were run in triplicates.

### Docking task

The second task was designed to be more diversity oriented as the goal is to generate as many high scoring compounds as possible for a dopamine type 2 receptor docking target (DRD2). The docking component was set up using DockStream[25] with a Glide backend[26]. The PDB entry id 6CM4[27] PDB file was downloaded from protein databank[28] and prepared for docking using Schrodinger Glide[26]. The DockStream component was set up with a reverse sigmoid transformation with a high score of -1 and a low score of -11 and a k parameter of 0.25. The molecular weight was restricted via a second scoring component used as a penalty, with a double sigmoid transformation with a high of 500 and a low of 0 Dalton. The two components were each given a weight of one and combined as a product for the final score. As before, experience replay was included with a memory size of 100 and a sample size of 10. A diversity filter[23] was employed with using scaffold similarity with a bin size of 35, a minimal similarity of 0.4 and a minimal score of 0.5. The diversity filter penalizes the agent by setting the score to zero if either the exact molecule has been sampled before or the scaffold has been seen a set number of times (here 35). 500 steps were used for each run (roughly 32,000 scoring function evaluations), and all experiments were made in triplicates.

As for the previous tasks, hyperparameter scan experiments were set up where augmentations were varied ([1, 2, 5, 10, 25, 50, 100]) or the learning rate was varied by multiplying the default with a defined factor ([1, 2, 5, 10, 25, 50, 100]).

### Augmented AHC

Finally we wanted to see if augmentation could also be used to enhance other generative algorithms and we thus implemented the augmented hill-climb (AHC) algorithm[12] in Diania, in both a standard and augmented form. For the augmented AHC we took the top-k scoring compounds from the generation, augmented the SMILES and used these for reinforcement learning a set number of times before generating new sequences with the agent.

The algorithms compared were: 5x SMILES augmentations, AHC with 5x SMILES augmentations, AHC and Reinvent 2.0. All experiments had the same goal, to generate DRD2 active binding molecules by optimizing a score towards a DRD2 QSAR model.

The QSAR model was trained on DRD2 binding active and inactive molecules from the ExCAPE-DB[30] database. All compounds with a pXC50 value above 5 for the DRD2 target were selected as actives, and a 5x larger selection of inactives was sampled randomly from compounds annotated as inactive on DRD2. The training and test set were evenly split using random selection. The model used was a C-support vector classification from scikit-learn[33] version 1.0.2 trained on count-based ECFP fingerprints with 2048 bits and radius 3, calculated with the Morgan fingerprint algorithm in RDKit.[34] The model parameters were tuned by running the RandomizedSearchCV tool from scikit-learn. The scoring selected was "f1\_micro", the number of iterations set to 50, CV to 3, and the limits for the Gamma parameter were [-5, 0] and for C were [-1, 3]. The hyperparameters values obtained from the tuning were: C set to 29.310978 and Gamma 0.00652. These parameters were then used to retrain on the entire training set and the performance was calculated on the external test set.

All the generative runs were performed without inception nor experience replay, with identical Murcko scaffold diversity filter with a bucket size of 25 and a minimal score of 0.4 The scoring function was composed of two elements: a molecular weight restraint with a weight of four and a QSAR component with a weight of six. The molecular weight restraint was modeled with a transformation type of double sigmoid, with a high limit of 620 and a low limit of 180. The batch size was 128 SMILES, the learning rate was set to default 0.0001, and sigma was also given its default value of 128. Finally, the margin threshold was fixed to 50 and the prior was as previously the random.prior.new obtained from the Reinvent Community repository[24]. The experiments were run for 500 steps in triplicates.

Extra hyperparameters had to be defined for those runs using SMILES augmentations or AHC. In the case of the runs with SMILES augmentations the number of augmentations was set to five. For the runs with the AHC implementation, the parameter top-k was 0.5. This is the fraction of generated molecules which score will be included in the loss and backpropagated to the agent.

For all runs the average score, the SMILES validity of the generated SMILES, as well as the number of molecules surpassing the minimal score of 0.5 was logged. The log files were analyzed to obtain the first step where a threshold similarity was passed or when the target compound was generated.

The yield of a generative run is the amount of unique and valid well-scoring compounds obtained usually expressed as a percentage of the number of generated SMILES strings. The yield was analyzed in more detail by calculating the yield fraction at different scores and plotting the results. The internal diversity of the generated unique molecules with a score above 0.5 was calculated with the IntDiv1 metric from the Moses benchmark.[29] For comparison the internal diversity of the DRD2 actives from ExcapeDB[30] was calculated after removing stereochemistry and filtering away

duplicates. The coverage of the chemical space was analyzed visually with Chemcharts[31], using standard settings with a joint UMAP[32] embedding of fingerprints (RDkfingerprint), calculating the cosine similarity between the datasets and subsequently plotting the individual datasets as hexbinned charts. The triplicate runs were pooled before dimensionality reduction and plotting.

## Results

### Similarity Task - Increasing Augmentation

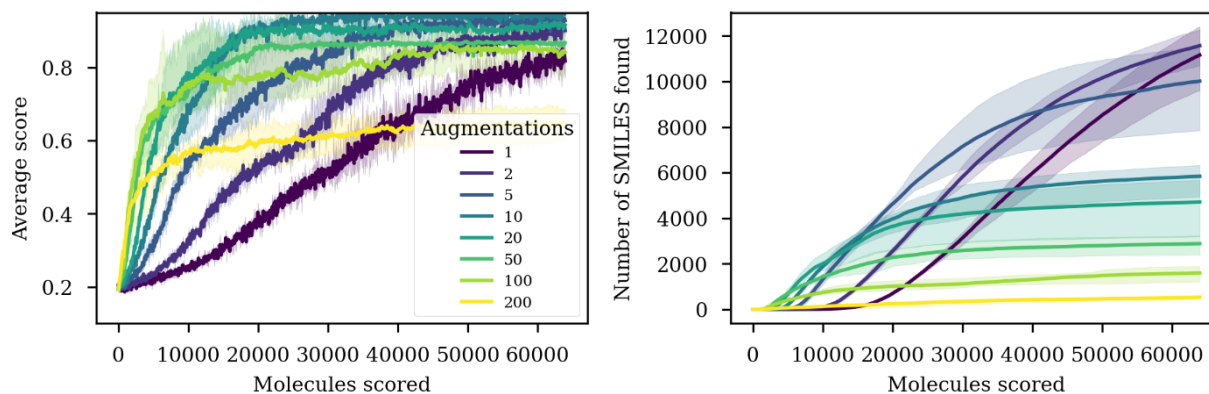


Figure 2: The effect of augmentations on the efficiency of the similarity task. LEFT: Using a larger number of augmentations leads to a marked effect on the efficiency of the search as evident from the diminished number of steps to reach scores over 0.8. However, the highest numbers of augmentations lead to an earlier and lower plateau. RIGHT: The effect of augmentations on the number of different SMILES generated surpassing the threshold score of 0.5. A higher number of augmentations leads to obtaining an earlier rise in the number of SMILES but is in the long run detrimental for the diversity of the generated SMILES as indicated by the plateauing and diminished rate of novel SMILES generation. Curves are mean of triplicate experiments with maximum and minimum shown as shaded area.

Augmentations leads to a marked increase in the efficiency of the generation, as higher similarities are obtained in a fraction of the molecule score evaluations of the run without multiple augmentations (Figure 2 left panel). However, the highest number of augmentations leads to a lower max score obtained at the plateau. Keeping the number of inner-loop augmentations at 10x, leads to both a high efficiency as well as a high maximum score at the plateau. This is also reflected in the number of SMILES surpassing the threshold shown in Figure 2 right panel. Here, a high number of augmentations do indeed lead to a faster rise in the yield of SMILES surpassing the threshold, but also lead to faster plateau, indicative that the same high scoring SMILES are repeated (mode collapse). The optimal number of augmentations thus depends on how long the run is intended to be. If there is a need for early return of some high-scoring SMILES, (10,000 molecules scored as in the proposed efficiency benchmark[17]), the optimal is around 10x augmentations, whereas if more patience and resources can be used, lower numbers of augmentations are optimal. On the other hand, it may not be fair to judge a run configured for exploitation with a diversity-oriented metric such as the yield of SMILES obtained which surpass the defined scoring threshold. The numbers of valid SMILES generated are in the high nineties and seems slightly higher for a higher number of augmentations (Supplementary Figure 1).

A summary of the steps when the runs with varying level of augmentation were solved are shown in Table 1 upper half. Here, three different definitions of a solved task are applied, when the target compound is generated, or the average score passes 0.5 or 0.8. If medium scoring compounds are wanted fast (the 0.5 threshold), the optimal strategy is to use many augmentations, whereas if more high scoring compounds (>0.8 or target generated) are wanted, a more moderate number of augmentations around x10 is optimal. The fastest run to re-find the target compound is with 100x augmentations using 73 steps, but this high setting also leads to more instability in the solution, as only one out of the three repeated runs found the target within 1000 steps.

Table 1: Steps until Similarity task were solved or passed an average score. Solved is when the exact target is obtained. Mean of solved is only including the runs that were solved, whereas mean is of all runs using the max number of steps for unsolved runs. The number of > characters denote how many runs were not solved. i.e., >> means two runs out of three weren't solved). Bold marks lowest numbers per column or both the augmentation scan and the learning rate scan.

x lr	x aug	Similarity >0.5		Similarity >0.8		Solved	
		Mean	Mean of Solved	Mean	Mean of Solved	Mean	Mean of Solved
1	1	414	414	781.3	781.3	251	251
1	2	260.3	260.3	550.3	550.3	320	320
1	5	133.3	133.3	375	375	242.3	242.3
1	10	93	93	<b>194</b>	<b>194</b>	<b>131.3</b>	131.3
1	20	63.7	63.7	172.7	172.7	>395.0	92.5
1	50	40	40	222.3	222.3	>>>1000.0	NAN
1	100	<b>39</b>	<b>39</b>	427	427	>>691.0	<b>73</b>
1	200	62.7	62.7	>>>1000.0	NAN	>>>1000.0	NAN
2	1	251	251	535	535	<b>214.3</b>	214.3
5	1	140	140	444	444	>728.7	593
10	1	103	103	<b>276</b>	<b>276</b>	365	365
20	1	89.7	89.7	348	348	>>758.3	275
40	1	<b>67</b>	<b>67</b>	>>745.7	237	>>694.7	<b>84</b>
60	1	95.3	95.3	>>>1000.0	NAN	>>>1000.0	NAN
80	1	>408.7	113	>>>1000.0	NAN	>>>1000.0	NAN
100	1	191.3	191.3	>>>1000.0	NAN	>>>1000.0	NAN

The effect of doing multiple updates could in principle also be that the default learning rate is not optimal for efficiency, and the multiple smaller weight updates mimics a higher learning rate. The similarity search runs were repeated with different learning rates. Figure 3 left panel show that increasing the learning indeed influences the efficiency on obtaining high scoring compounds and as for the increases in augmentations, there is an optimum whereafter the average score is finding a plateau at a lower average score. The variations of the runs are larger for higher learning rates, and this instability is reflected in the large number of runs that fails to find solutions as evidenced in Table 1, lower half. This instability at higher learning rate is also seen in Figure 4, where the SMILES validity is dropping markedly for the highest learning rates, but surprisingly recovers as the agent learn to generate valid SMILES even under the extreme neural network weight updates. Interestingly, the number of SMILES found are not as affected as for the increase in augmentation, but the variability in yield is higher, especially for the high learning rates. (Figure 3 Right panel)

It was further investigated if it is indeed the augmentations and not simply the many smaller updates to the agents' weights, an experiment was run with several repeats in the inner loop with the default learning rate but reusing the sampled SMILES sequences rather than augmenting them. The plot in

Supplementary Figure 4, shows that this also influences the efficiency, but with a much higher propensity for reaching a suboptimal plateau in the generations. Even at the lowest settings of the repeats, the yield of SMILES is lower than for the augmented runs (compared to Figure 2). The efficiency is however higher for using the sequences as sampled as is evidenced for the faster increase of using only one repeat as sampled compared to the use of one augmentation (Supplementary Figure 4 and Figure 2). However, using as little as three augmentations is more efficient than using one sequence as sampled (results not shown).

#### Similarity Task - Increasing Learning Rate

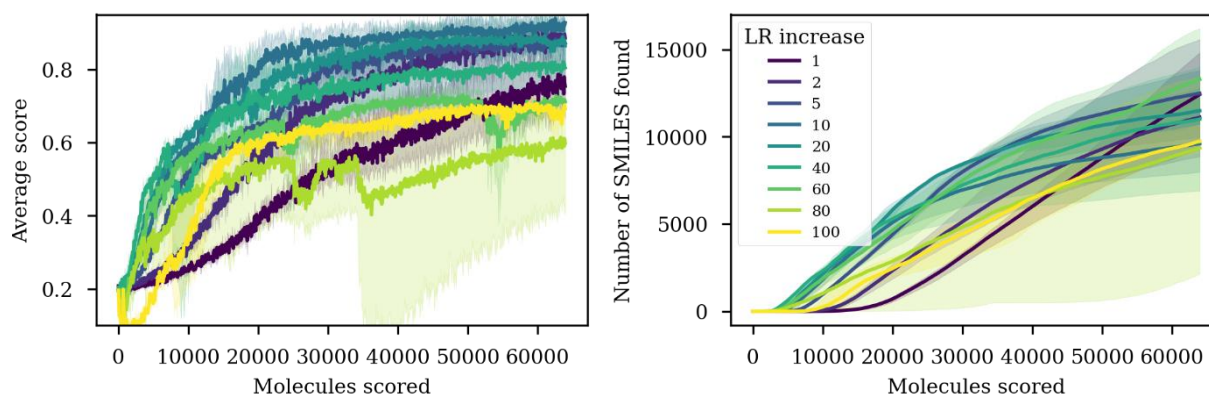


Figure 3: Effect of increasing the learning rate for the similarity task. LEFT: efficiency of the score optimization. Higher learning rate leads to obtaining good scores faster, but a too high learning rate leads to instability. RIGHT: The number of SMILES obtained above threshold score 0.5.

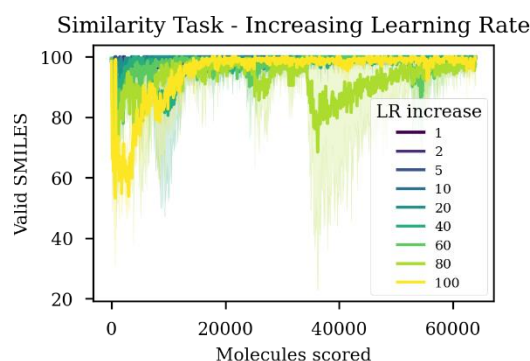


Figure 4: Effect of increasing learning rate on SMILES validity. The highest settings lead to instability and a lower fraction of valid SMILES. Surprisingly, the agent learns to recover from this.

A grid search experiment was conducted where combinations of learning rates and number of augmentations were tested. Figure 5 left panel shows a heatmap of the number of steps necessary to bring the mean similarity over 0.5. The plot highlights the synergy between increasing the learning rate and increasing the augmentations. If a higher learning rate is chosen, a lower number of augmentations is needed to bring the average score to the same level for the same number of steps. However, as shown in Figure 5 right panel, the risk of getting unsuccessful runs quickly increases when combining higher learning rate with a higher number of augmentations.

The results of the grid search are shown fully in Supplementary Table 1. The fastest stable solution is obtained in 122 steps with an augmentation of x2 and a learning rate increase of x3, where all three runs successfully found the target molecule. The fastest single run to generate the target was found

in 44 steps with an augmentation of x5 in combination with a learning rate increase of x7, but this was only obtained for one out of three runs, where the others failed to find the solution in 500 steps.

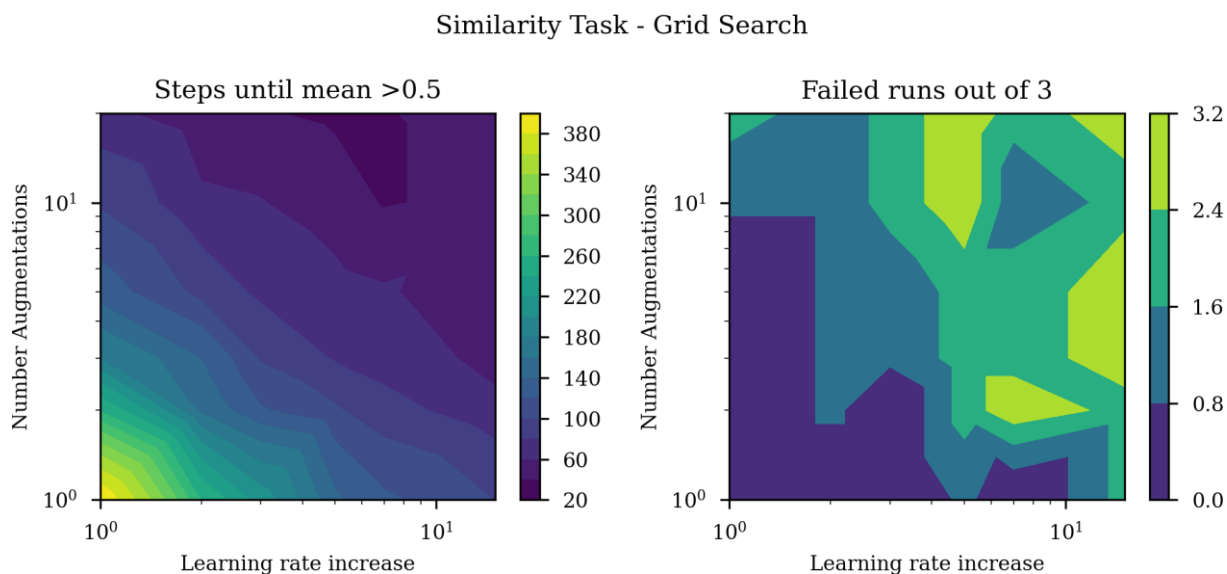


Figure 5: Effect of combining increased learning rate with increased number of augmentations. LEFT: Heatmap of the steps needed to obtain an average score of 0.5 or above for combinations of learning rates and number of augmentations. RIGHT: Number of runs that failed to find the solution for different combinations of learning rate increase and number of augmentations.

### Docking Task

For a more explorative task an automated docking and scoring with a dopamine type 2 receptor docking target (DRD2) receptor was used. The aim was to generate as many and diverse, but good docking molecules. A molecular weight penalty was added to the compound scoring function and a diversity filter was used during the run, to keep the size of the molecules reasonable and encourage exploration. Figure 6 show the outcome of the docking task with different number of augmentations. Like the previous task, the augmentations influence the effectiveness with which the average docking score increases, but unlike for the similarity task, the efficiency has an optimum at 100 augmentations which also obtains the largest average score on the plateau. Some of the curves has an interesting spike in the beginning, where the average score increases rapidly, followed by a slight drop and a recovery in the long run. We interpret this as the effect of the diversity filter, that stops overexploitation. However, even though the average yield seems to get best at 100x augmentations, the yield of SMILES is lower for this number of augmentations (Figure 6 right panel). The yield of unique SMILES surpassing the scoring threshold is highest around 5x-10x augmentations with a higher variability in the 10x augmentations run, than in the generative runs with 5x augmentations. The validity is in the high nineties for all runs (Supplementary Figure 2).

Varying the learning rate also influenced the efficiency of the reinforcement learning for the docking task, where higher learning rates allowed the reinforcement learning to find better scoring molecules faster (Figure 7) for all increases but the highest, which also show a large variation between the runs. This may in part be due to the instability of the run where validity of the SMILES drops markedly, as previously observed for the increases in learning rate for the similarity task (Supplementary Figure 3). However, in contrast to the findings for the learning rate experiments (c.f. Figure 6 right panel), the final yield of SMILES is immediately and negative affected for all learning rate increases (**Error! Reference source not found.** right panel) even though yield at intermediate run lengths are improved.

## Docking Task - Increasing Augmentation

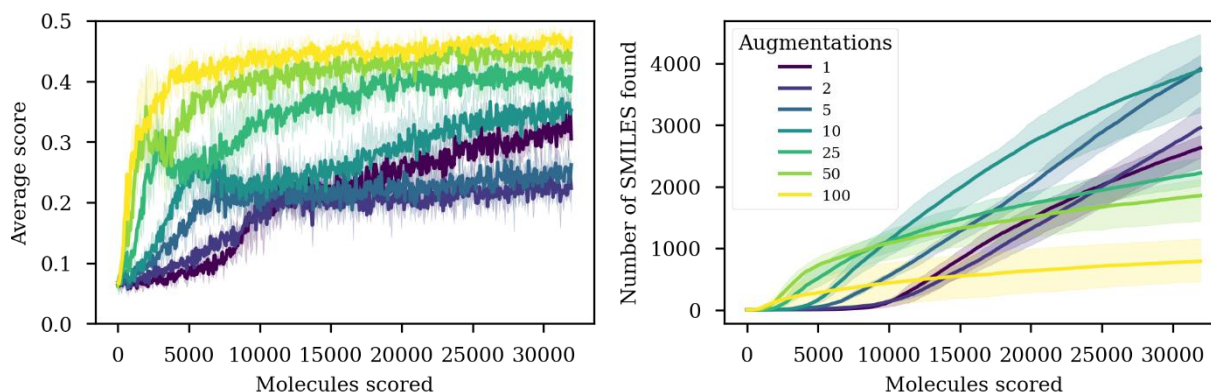


Figure 6: Effect of increased number of augmentations in the Docking task. LEFT: More augmentations lead to higher optimization efficiency. RIGHT: The number of SMILES found initially increases with higher number of augmentations, but the highest settings lead to lower number at the end.

## Docking Task - Increasing Learning Rate

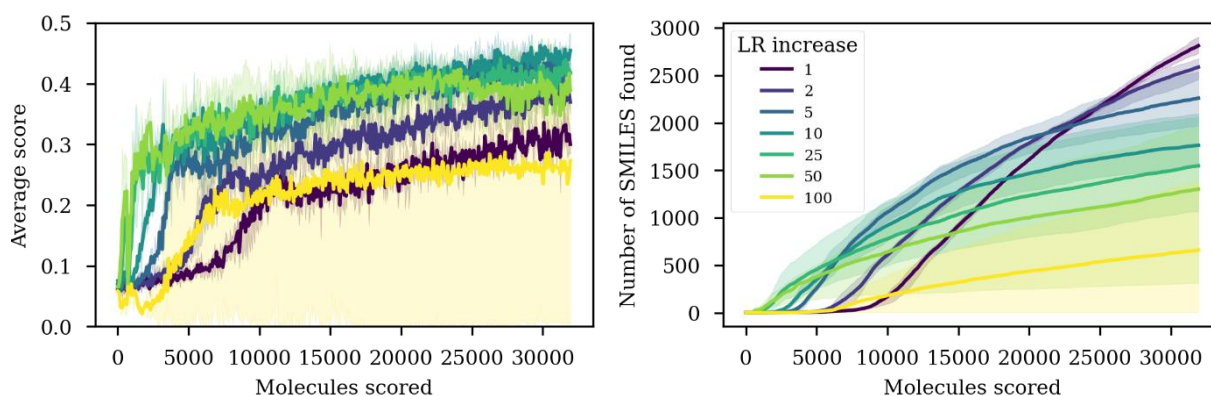


Figure 7: Effect of increased learning rate on the Docking task. LEFT: Medium learning rate increases leads to higher optimization efficiency. RIGHT: The number of SMILES found initially increases with higher learning rate, but all increases lead to a lower number of obtained unique SMILES at the end.

## Yield and diversity of the generated compounds

As we are often not only interested in the top scoring compound but would rather have several diverse compounds and series for postprocessing, the yield and diversity of the generative process is of interest. The yield is the number or fraction of generated unique compounds that pass a given score. The yield curves in Figure 8 and Figure 9 follows the yield fraction over different score thresholds, for augmentation and learning rate increases, respectively. For increases in learning rate the yield fraction drops over the entire range of possible score thresholds, whereas it for the augmentations increases for modest number of augmentations before dropping again for the highest settings.

### Docking Task - Increasing Augmentation

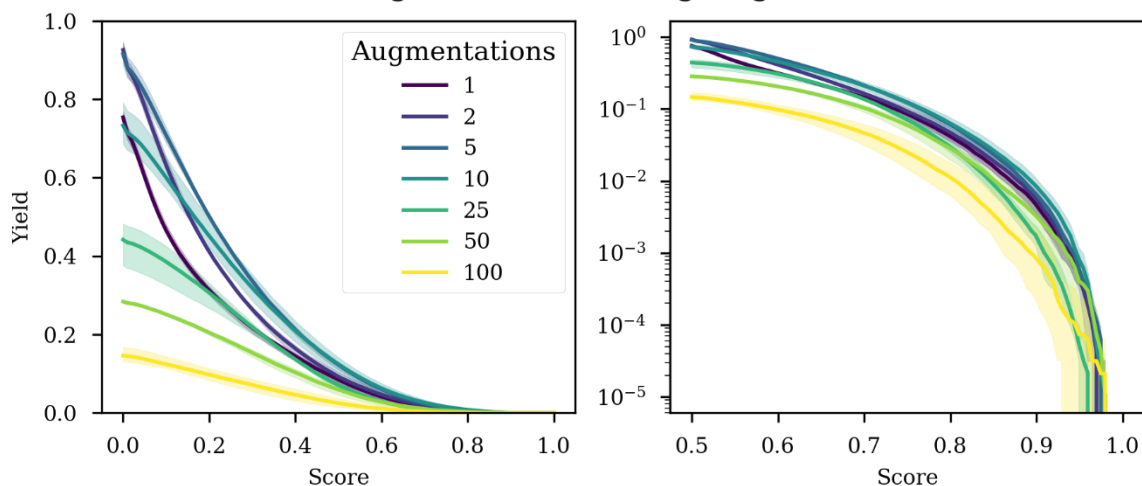


Figure 8 Yield fraction curves for the augmented runs of the docking task. Left is shown the total yield curves, whereas right shown the compounds scoring over 0.5 on a semi-logarithmic plot. For x2-5 augmentations the yields are higher for most score thresholds, but the yield drops with a higher number of augmentations.

### Docking Task - Increasing Learning Rate

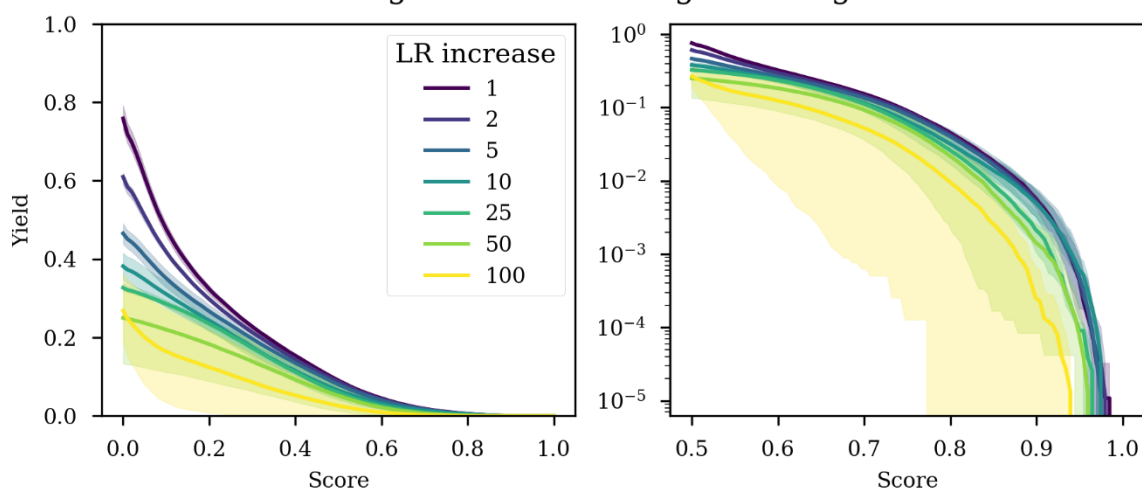


Figure 9 Yield fraction curves for the runs with varying learning rate. Left shows yield for all scores, where right is shown for compounds scoring over 0.5 in a semi logarithmic plot. Curves are mean of triplicate runs with min and max as the shaded area. Yield drops with increasing learning rate across the entire range of scores, and lead to higher instability for largest increases.

The diversity was further quantified with the internal diversity measure from the Moses benchmark[29](IntDiv1) and compared with the internal diversity of the DRD2 actives. The internal diversity measures the average fingerprint Tanimoto similarity between the compounds in the dataset, and is a quality that is characteristic of a single dataset, rather than a comparison between prior and generated datasets that are most used in generative metrics.[16], [29]

Figure 10 shows how the internal diversity varies for the different configuration of hyperparameters. With augmentation the internal diversity increases to reach a maximum at five augmentations for then dropping slightly towards the highest settings, that also show greater variability. The increase in learning rate leads to a less marked increase in internal diversity, but the largest variation between the triplicate runs for the highest increases. The IntDiv2 metric showed qualitatively the same profile, although with lower absolute values (results not shown). The results thus indicate that we can both

increase efficiency by increasing the number of augmentations to a certain degree, and at the same time increase the diversity of the output, whereas this is less likely to be the case by increasing the learning rate.

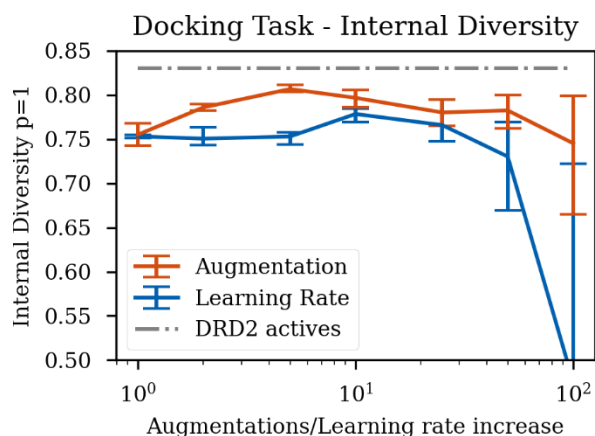


Figure 10: Mean internal diversity of the docking task generative runs. Error bars are min and max of the triplicates.

The coverage of chemical space was further examined visually with the ChemCharts[31] package. Using UMAP[32] for defining a common 2D space, the distributions of the generated compounds can be visualized in 2D hexbin plots as shown in Figure 11 and Figure 12 for the augmented or learning rate increases, respectively. Interestingly, the generation with moderate augmentation seem to sample the same areas, although to slightly different degrees in the various areas of chemical space. Moreover, moderate settings with x2-x10 times augmentation seem to lead to a more spread-out sampling, which is in accordance with the internal diversity metrics plotted in Figure 10. The increase in learning rate seem to gradually lead to partial mode collapse and an overfocus of one or few areas of the generated chemical space (Figure 12).

The similarity between all the datasets was compared using the cosine calculations provided by the ChemCharts package and is shown in the heatmap in Figure 13. Standard Learning rate and an augmentation of one, have a cosine similarity of 0.89. The runs have the same settings and apparently also sample the same space to a large degree. However, the largest similarity is between the augmentation runs x2,x5 and x10, which indicate that the use of augmentation increase reproducibility of the generated space, which may seem surprising as this is also the settings where we observe the largest diversity (c.f Figure 10 and Figure 11). The similarity to the runs with an augmentation of x1, is however lower, which indicates that these runs is sampling a slightly different space, or some areas to a different degree, where Figure 11 top row seems to indicate the later as the overall spread in chemical space is similar, but intensities are different. For the generation with learning rate increases, we observe a gradual diminishing of similarity, with the smallest increases being the most similar. Higher learning rates thus leads to less reproducibility in the outcome. Both learning rate and augmentation increases at the extreme level of x100 are outliers with the cosine distances to the rest of the datasets, probably due to the mode collapse as is also evident from Figure 11 and Figure 12 bottom rows.

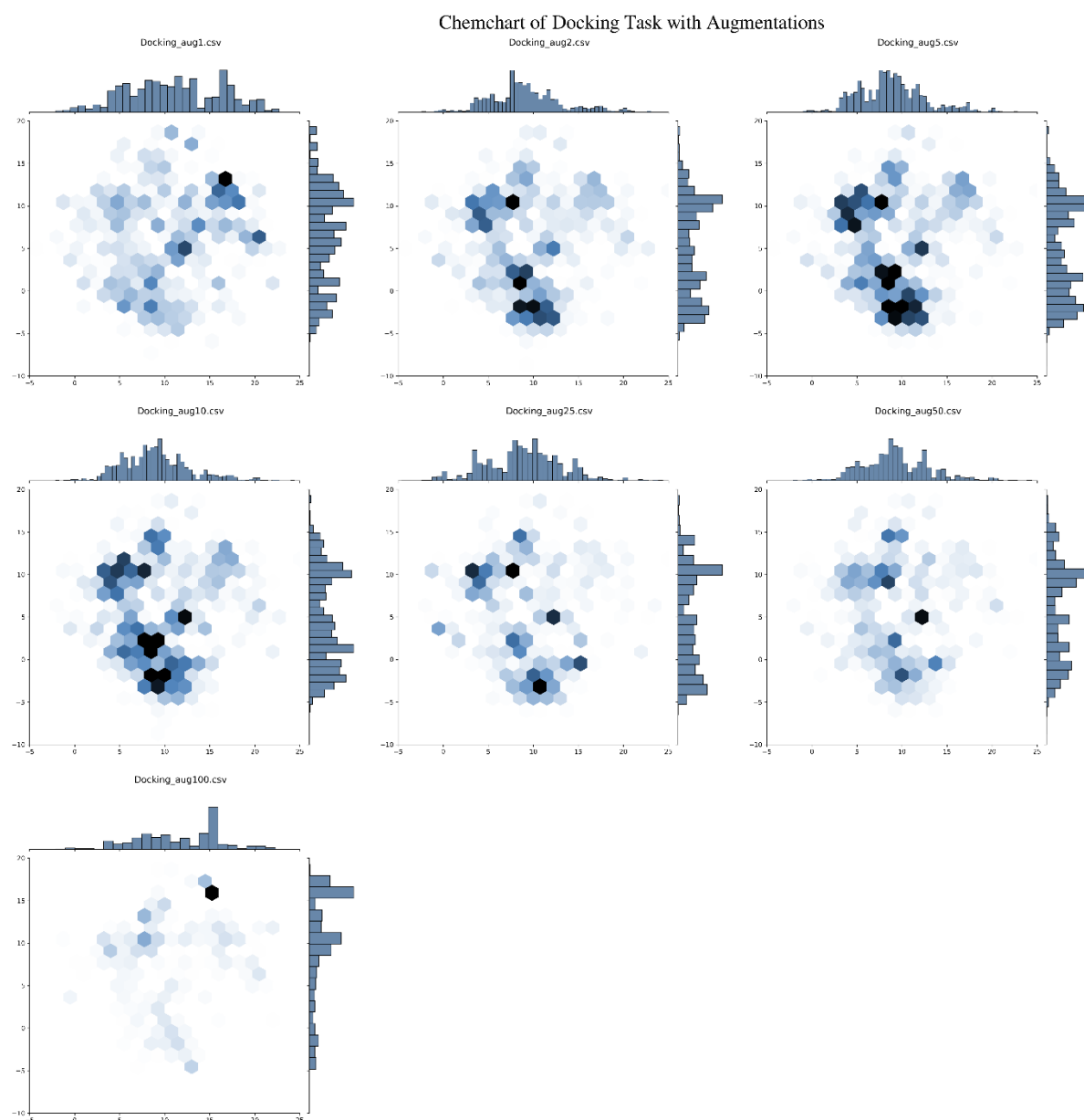


Figure 11 Chemcharts hexbin plot visualization of the distribution of sampled molecules from pooled triplicate runs of the docking task with different levels of augmentation. Augmentations increase left-to-right, top-to-bottom. Augmentations of between 2 and 10 sample very similar spaces with a high diversity.

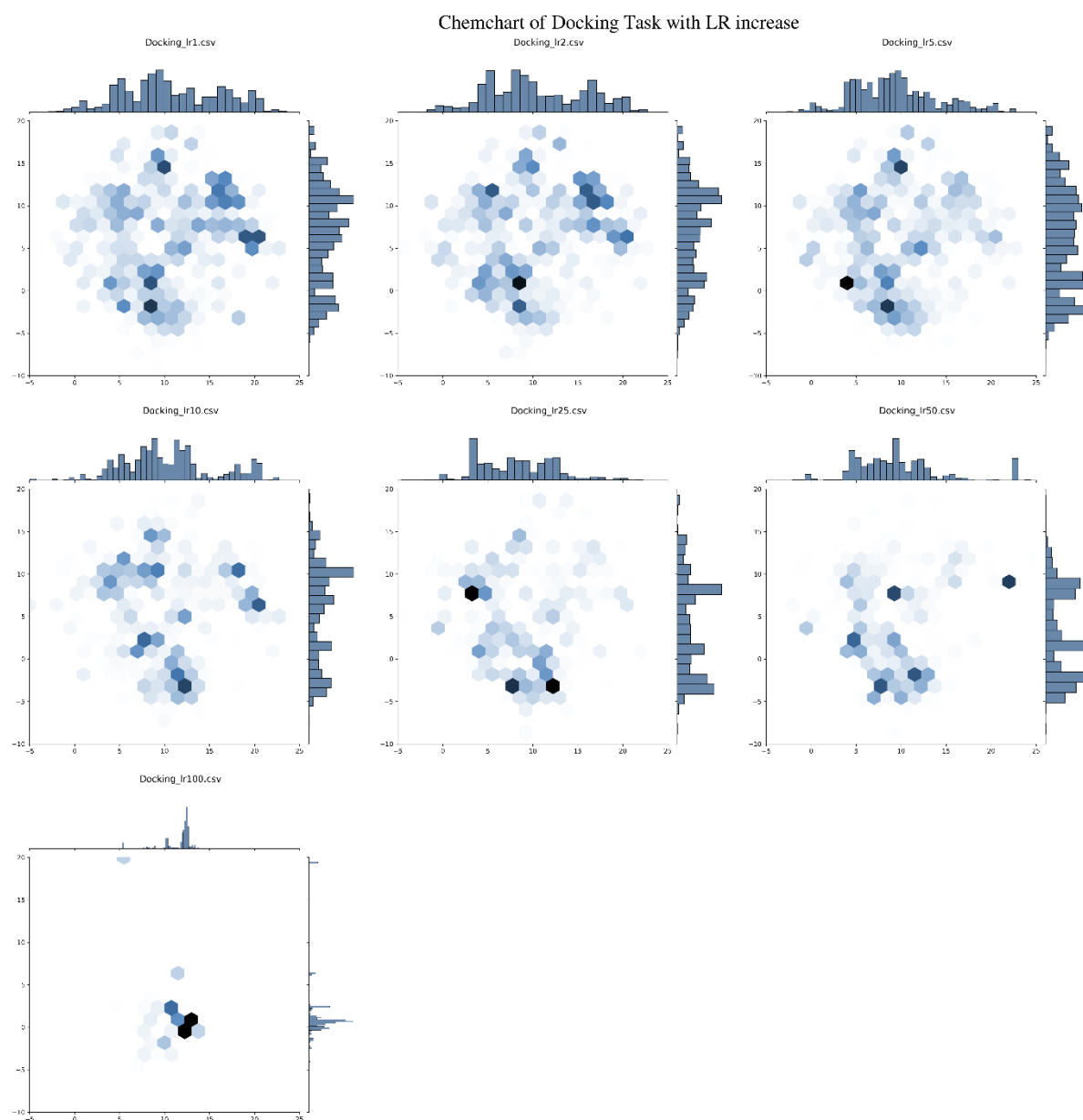


Figure 12 Chemcharts hexbin plot visualization of the distribution of sampled molecules from pooled triplicate runs of the docking task with different learning rate increases. Learning rate factors increase row wise from x1 (top-left) to bottom.. The learning rate increases of 1x to 5x seem to sample the same areas, but with different intensity. As the learning rate increases, fewer and fewer areas seem to be sampled, until there's a full mode collapse at 100x learning rate increase.

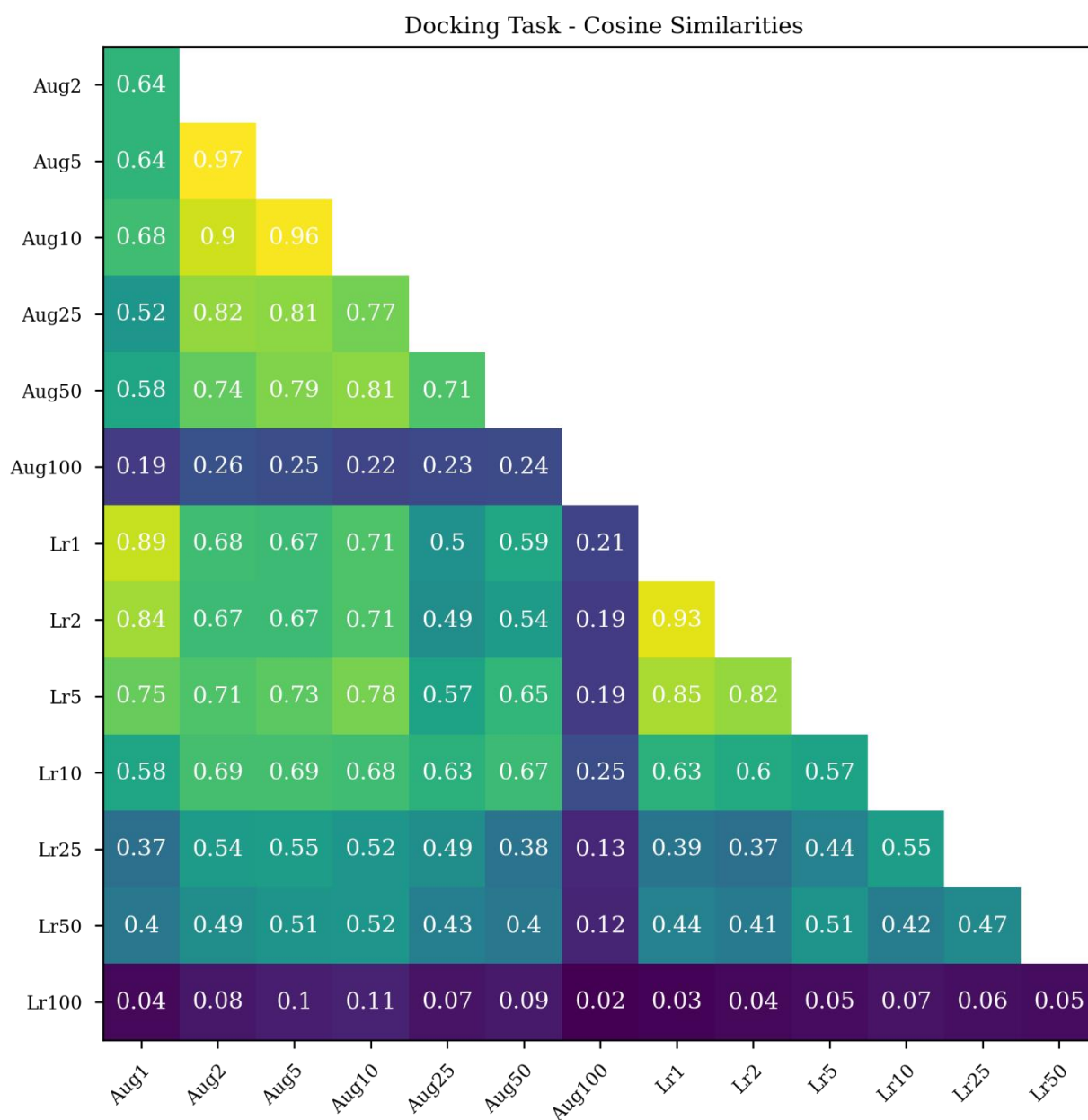


Figure 13: ChemCharts cosine similarities between the pooled triplicates. Light yellow color indicates a large similarity in the sampled chemical space, whereas dark purple indicates a low similarity.

## Augmented AHC

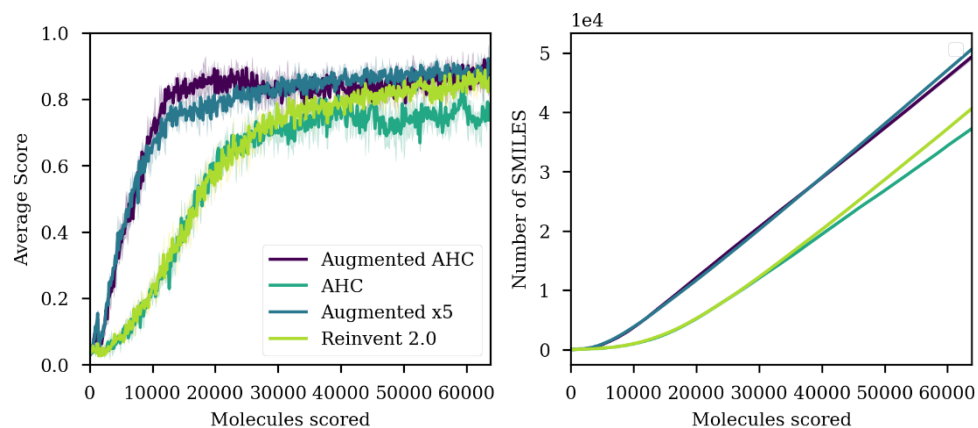


Figure 14: Effects of the different algorithms as an average of the triplicates. LEFT: Average score of molecules produced as a function of molecules scored. RIGHT: Number of molecules produced with a score above 0.5 as a function of molecules scored. The augmented versions perform better in both.

The augmented hill-climb and standard reinforcement learning as well as their augmented counterparts were tested on optimization towards a DRD2 QSAR classification model. The model was trained on known active and inactive compounds and obtained good performance metrics on the held-out test set: F1 score: 0.99, Matthew's correlation coefficient: 0.96 and the balanced accuracy: 0.98.

The augmented strategies reached higher scores faster than the non-augmented ones as it can be seen in the right panel of Figure 14. The Augmented AHC model was the first one to reach average scores above 0.8, but the augmented only algorithm started to achieve higher average scores at around 30,000 molecules scored. Also, both augmented strategies reached convergence much faster than their non-augmented counterparts. Furthermore, the AHC strategy performed worse than Reinvent 2.0 as it didn't optimize faster as well as converged to lower scoring values.

Regarding the number of SMILES found as a function of molecules scored, the differences between the algorithms was parallel to the findings for the average score. Figure 14 shows that the augmented algorithms produced a much higher number of SMILES than the non-augmented ones. Again, the Augmented SMILES model was the one that generated the larger number of SMILES and the standard AHC the one that produced the lowest number. The AHC algorithm started to get productive at around the same steps scored as reinvent, but the rate of generating new molecules was lower.

Overall, the augmented strategies achieved higher scoring molecules faster and were also able to produce a larger number of molecules than their non-augmented counterparts.

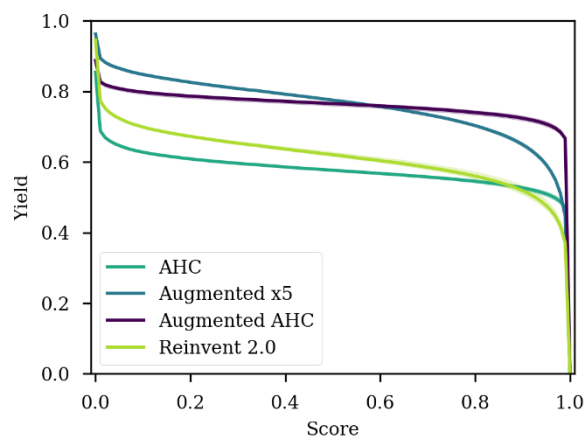


Figure 15: Yield fraction curves as a function of the score. Higher yield means a higher number of unique smiles with a greater score.

Figure 15 left panel shows the average yield over all replicas of the different model runs as a function of the threshold score. In this case, the yield was defined as the number of SMILES above a certain score divided by the total number of smiles produced. Therefore, a yield curve containing higher values means that a larger percentage of the total SMILES produced have higher scores. Augmented strategies performed better again, as they showed higher yield values. This is not surprising, as these strategies had better average scores for the whole run than their non-augmented counterparts. On the other hand, the AHC versions of the algorithms achieved a higher fraction of top-scoring molecules, than their non-augmented counterparts, evidenced by the cross-over of the curves and the steepness of the curves close to 1.0.

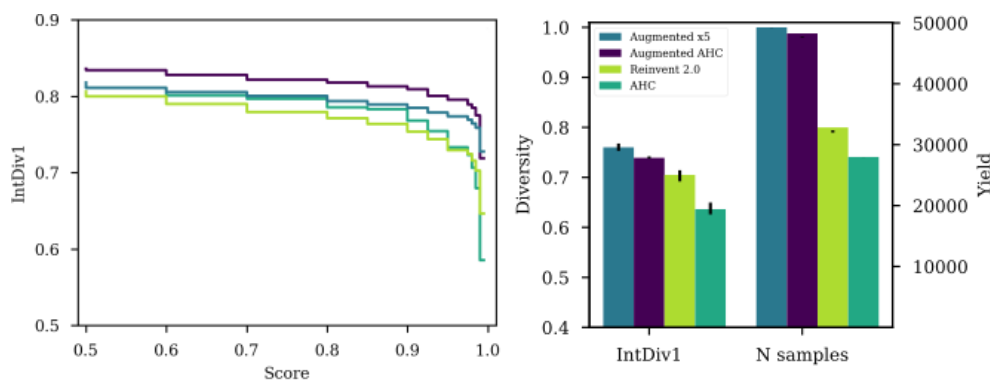


Figure 16: Properties of the generated datasets from the four generation algorithms. LEFT: Intervallic Internal diversity as a function of the score. The internal diversity (IntDiv1) was calculated with MOSES Benchmark. RIGHT: Overall internal diversity of unique molecules with a score greater than 0.5 and number of unique molecules generated. The error-bars show the min and the max of the triplicate runs.

The right panel of Figure 16 shows the total internal diversity of unique molecules with a score greater than 0.5. The average values over the three replicas were: 0.76 for the Augmented SMILES, 0.74 for the Augmented AHC, 0.7 for Reinvent 2.0 and 0.63 for the AHC. The augmented strategies not only reached higher scores faster, but their molecules produced were more diverse. In this case, the Augmented SMILES had the highest overall diversity. Note that the AHC versions had a lower internal diversity than their augmented counterpart, being the non-augmented AHC strategy the one with the lowest diversity and lowest number of unique molecules generated.

Similarly, the left panel of Figure 16 shows the average internal diversity across different score intervals, as example, the first step is the internal diversity of unique molecules generated that have

score in between 0.5 and 0.6. As the augmented algorithms made generated molecular datasets with a higher total internal diversity and higher yield, it is not surprising that they performed better here too. It is worth noting that despite AHC strategies obtaining higher internal diversity over most steps, in the last steps closer to the maximum score 1.0, the non-AHC counterpart strategies get a higher internal diversity. Thus, the AHC strategies produced less diverse compounds with scores really close to 1.0, which is also the interval where AHC algorithms get a much higher yield than the non-AHC counterparts (c.f. Figure 15), which explains that the total diversity is lower for all molecules with a score above 0.5 (Figure 16 Right panel).

Taken together, the results show that not only the augmented strategies have a greater overall diversity, but they also have a greater diversity in higher scoring compounds (Figure 15 and Figure 16).

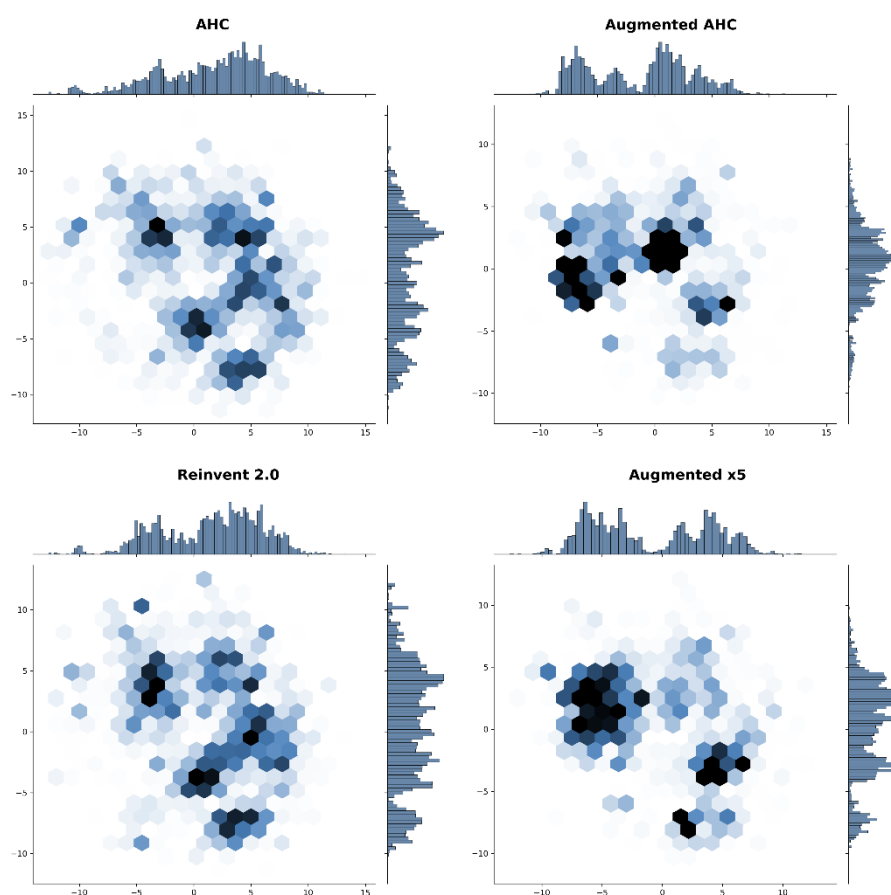


Figure 17: Normalized Chemcharts with hex visualization of the distribution in chemical space of the molecules generated by the different algorithms. The two non-augmented variants appear visualize similar. The augmented variants appear to sample fewer areas but cover more neighboring hex-bins intensely.

Figure 17 shows the 2D hexabin Chemcharts plots of the chemical space covered by the molecules generated with a score higher than 0.5 in all replicas of each experiment. All models covered similar areas within the chemical space but in this case the non-augmented strategies covered a wider region with less density. This may be because the augmented strategies were more likely to explore areas in more depth as they found high scoring molecules earlier in the generative runs, while the non-augmented ones were more likely to cover areas more lightly while still searching for higher scoring molecules. Despite the non-augmented strategies covering a slightly wider area of the

chemical space, the internal diversity plots shows that the augmented strategies anyhow had a higher diversity (Figure 16). The augmented runs seem to intensely sample neighboring hexbins more intensely. Interestingly, the algorithms seem to group as non-augmented runs are more similar than to their augmented counterpart. This trend for grouping was also observed for the docking runs (c.f. Figure 13). The standard Reinvent 2.0 and non-augmented AHC strategies were the ones to cover the most similar areas of the chemical space, with a Chemcharts cosine similarity value of 0.79. The augmented SMILES model had a similarity in the range of 0.44 to 0.48 with all other runs, whereas the augmented AHC appeared most dissimilar to the datasets generated with non-augmented algorithms, with cosine distances of 0.27-0.28.

Overall, it is clear from the results shown in Figure 14-16 that the AHC strategy performed worse than Reinvent 2.0 with respect to generated yield of SMILES as well the internal diversity. The Augmented x5 strategy was the one that performed the best with regard to overall yield and diversity, except that the yield of perfectly scoring molecules were lower than for the augmented AHC. Thus, AHC strategies lead to an increase in the fraction of perfectly scoring molecules, but a decrease in diversity, which can be counteracted by introducing SMILES augmentations.

#### Similarity to known DRD2 actives

The docking runs generated compounds without any ligand information in the scoring function, so the question arises if the generated compounds look anything like what we expect of DRD2 ligands. The generated compounds with a score over 0.5 from generative runs with standard settings or moderately increased number of augmentations or learning rate (both x5) were compared with known actives from the DRD2 dataset by calculating the pairwise Tanimoto similarity based on Morgan fingerprints. With the standard settings without increases in learning rate or number of augmentations, we identified two compounds with a similarity over 0.8 and 84 with a similarity over 0.7. Increasing the number of augmentations in the inner loop to x5, increases the number of compounds identified with a similarity over 0.8 twelvefold to 24, and the number of compounds with a similarity over 0.7 to 140. In contrast, the increased learning rate leads to a drop in the number of compounds above 0.7 similarity to 41, but still with two compounds found with a similarity above 0.8.

The most similar compounds from the x5 augmented run are shown together with their counterparts from the known DRD2 actives dataset in Figure 18. Given the large generative possibilities and the lack of structural guidance for the ligands that could come from a QSAR model, it is still possible to generate compounds with a structural similarity to known actives only by using a docking target. They seem on average small, and do not obtain the highest docking scores. This is likely because it may be easier to generate molecules with a high similarity when the compounds are both small. Many of the generated compounds (and the known actives), share features with the DRD2 receptors native ligand dopamine but with a locked aliphatic amine. The marked increase in the number of compounds with above 0.8 similarity indicates that the double loop augmented reinforcement learning also increases the capability to find similar compounds to the native and known active ligands

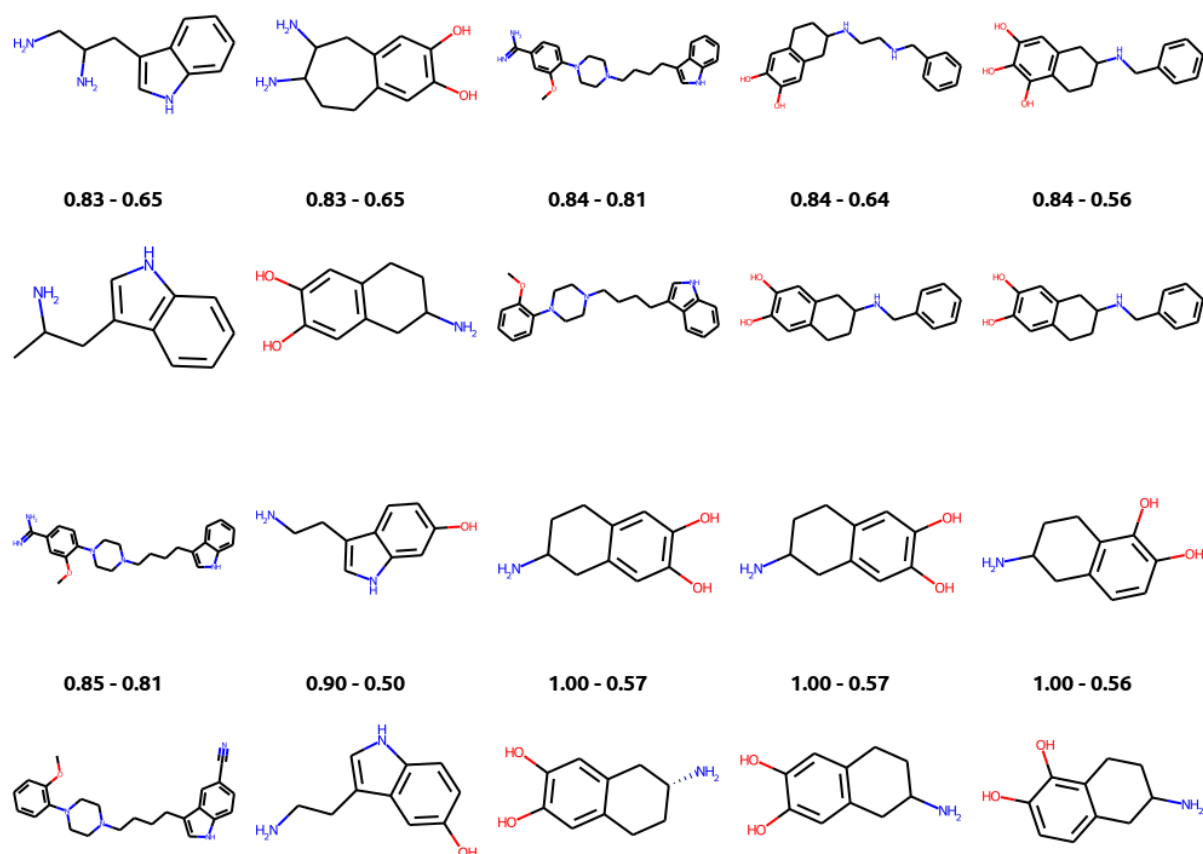


Figure 18: Generated compounds with maximum similarity to known DRD2 actives. Row 1 and 3 are generated compounds with their closest known active in row 2 and 4. Numbers are the Tanimoto similarity and the score.

## Discussion

Recent papers[12], [17] addressing the efficiency of molecular generative algorithms both had a focus on exploitation and efficiency as they focused on how fast good scoring compounds be obtained, but had less emphasis on the diversity and yield of the produced output. The reason may be, that it is easy to measure the exploitation with a single metric, but much harder to quantify the diversity and quality of the generated compounds. We have the latest years witnessed far too many papers showcasing, and competing on, which algorithm can most efficiently find the compound with the largest calculated penalized logP. This is however not a useful scenario in drug discovery, as we seldom want to maximize a given property, but rather need to balance a long range of, sometimes, conflicting properties of a molecule to make a drug candidate. Thus, most often generative de novo design in drug discovery is done with an aspect of exploration and diversity in mind, to get several different putative ligand series and ideas for continuous workup, such as filtering and prioritizing by criteria such as synthesizability in collaboration with project computational chemists and medicinal chemist. The generated compounds diversity thus also needs to be considered for a fuller view of the performance of the generative algorithm. As our results show, one tuning parameter such as learning rate can increase the efficiency as it is increased, but this is an immediately tradeoff with the diversity and final yields. The use of augmentation, however, seem to allow for both increasing the

efficiency as well as increase the diversity and reproducibility, making it particularly attractive for use in practical drug discovery scenarios.

The augmented Hill-Climb algorithm showed an impressive speedup of 45x fold on single-sample comparison and a 7.4 times larger efficiency when calculated on the average.[12] We have not in the same way analyzed the single sample efficiency, which is the ratio between steps when a single sample passed a given score threshold. However, we can estimate efficiency speedups by using the data in Table 1. For the threshold of 0.5 we see an approximate 10x larger efficiency at an augmentation of 40 times in the inner loop, whereas for the threshold of 0.8, this is around 4x using 10-20x augmentations. For the first step with solved, we have an approximately 2x increase in efficiency. Thus, the speedup efficiency number thus seem to depend heavily on which scoring threshold or criteria is used. Further, the augmented hill-climb study compared to the first version of Reinvent which struggled to see meaningful docking scores for a DRD2 docking target within 500 steps, where we in contrast start to observe marked improvements in docking scores of compounds after only 7500 molecules scored, which corresponds to around 120 steps. It thus appears that the baselines for the efficiency increases are not really performing similar, and the increases from the baselines are thus not comparable. The metric of efficiency increase on the sample-level is also something we would discourage, as it focuses too much on finding a single good scoring molecule, rather than also taking the average scores and diversity of the proposed molecules into consideration. Nevertheless, double loop augmented reinforcement learning seems competitive regarding average score efficiency speedups.

Given the impressive speedups reported in the preprint about the AHC algorithm[12], we were surprised to see the very similar performance when compared to standard Reinvent 2.0. However, it appears that the comparison in the paper was with the previous version of reinvent, as well as with a different setting of the sigma parameter. Basically, for most of the experiments in the preprint[12], reinvent failed to yield meaningful increases in the average scores. Thomas and co-workers also observed, that without a diversity filter, the AHC algorithms were prone to mode collapse. We included a standard diversity filter, but nevertheless see a tendency for the AHC versions of the algorithm to yield a higher fraction of perfectly scoring molecules, but with a lower internal diversity, which could indicate a beginning hyper-focus and mode-collapse.

Gao and Fu and co-workers made an extensive benchmark which focuses on optimization efficiency and used it to benchmark 25 methods across 23 various widely used oracle functions.[17] They limited calls up to 10,000 queries and measured the models' performances with the area under the curve (AUC). Interestingly, they found REINVENT 2.0 to be quite competitive, albeit with a tuned sigma value. Our experiments entirely compare to REINVENT 2.0 as a form of baseline and it is thus reassuring that our baseline is a strong one.

The benchmark measures performance across the methods are compared with AUC of the average of the top-10 solutions found per number of oracle calls. The task most like ours is the DRD2 oracle, which is a QSAR model of a DRD2 dataset. We thus in a similar fashion calculated the AUC-top10 of the QSAR task. We find the augmented RL and the augmented AHC have AUC values of  $0.9989 \pm 0.0003$  and  $0.9985 \pm 0.0004$ , respectively. However, we believe that this may be due to differences in the QSAR models dynamic range as the standard run also gets a high value of  $0.9977 \pm 0.0004$ , which is markedly higher than the  $0.945 \pm 0.007$  obtained in the PMO benchmark.[17]

In contrast to the recently proposed benchmark[17], we kept the sigma variable for the reinforcement learning fixed at the default 128. Changing this to a higher setting as Gao and Fu and co-workers did, could likely have opened for additional tuning of the efficiency, but the effect on the diversity and yield would have to be closely watched. Moreover, the quality of the proposed molecules could suffer[18], as the prior generator is given less weight. In contrast, no big change in

performance was observed for tuning sigma of Reinvent 1 with the intention to compare to the augmented hill-climb algorithm.[12]

On the other hand, 10,000 oracle calls correspond to approximately 150 steps with a batch size of 64. As shown in several of our experiments, the conclusion of the most efficient method varies with the length of the experiment. As example cutting the experiment with learning rate increases for the docking task at 150 steps, would have led to the conclusion that a learning rate increase of x5 would be the most efficient, where running the experiment for longer, show several cross-overs of the SMILES yield for the different settings and thus changes the conclusion on which algorithm is the most efficient (c.f. Figure 7). 10,000 function evaluations are also an order of magnitude lower than what we have applied in generative runs in practice. We would thus suggest running the benchmarks for longer and report the findings for different lengths of runs. This could better inform the decision on algorithm choice when taking the computational budget for oracle calls into consideration. Moreover, ten candidate proposals are in our experience far too little to progress with in further post-processing. It's an unfortunate drawback that the metrics are thus very focused on finding very few good scoring candidates leading to an overly focus on optimization, without considering the diversity and yield of the methods. The authors discuss this drawback and plan to address it in future work for a likely update of the PMO benchmark.

We were pleased to see that the method, even without any ligand-based scoring function, but just with a docking target could generate ligands similar to known actives. The barrier to get structural information for a given protein target is now much diminished due to availability of high-quality 3D protein structural prediction from algorithms such as AlphaFold2.[35] Thus, the way for an in silico pathway from target sequence to ligand seem within reach, although using the predicted protein structures for docking is not yet as good as with X-ray crystallographic data and may require further work[36]. However, it must be noted that our prior and thus agent are likely pre-trained on a large dataset which included SMILES strings from DRD2 datasets, which could result in the prior already having a propensity for generating ligands with these structures. The fraction of the DRD2 ligands in the dataset is however minuscule, so the effect is probably negligible and it has already been shown that even when removing known or similar ligands associated with the target, reinforcement learning can result in rediscovery of known actives[2], [37]

## Conclusion

Efficiency of reinforcement learning for optimization of molecular generation can be increased with both increasing the learning rate (bigger updates per step), or via augmentations (multiple smaller updates along different generation paths to the same molecules). However, too much increase in efficiency gives lower SMILES yield and/or variability for both learning rate increases and number of augmentations but using augmentation at a moderate setting (x5-x10), both increases efficiency as well as increases diversity of the generated output, in contrast to increasing learning rate, where final yield already drops with a factor two increase from the default setting. Further, increasing augmentation to x2-x10 increases the reproducibility in the sense that the same chemical space is sampled, although the molecules are not the same between the repeats of the runs. We thus recommend using around x5 augmentations for explorative runs, where strictly exploitive scenarios can go higher to x10 augmentation.

## Acknowledgements

We want to acknowledge the data science team at Odyssey Therapeutics for helpful feedback and discussions, and especially the Reinvent expertise of Dr. Atanas Patronov and Dr. Kostas

Papadopoulos. We also want to acknowledge Sophie Margreitter for the helpful discussions about ChemChart code modifications.

## Conflicts of Interest

Authors are employees at Odyssey Therapeutics, which has a commercial interest in utilizing generative modelling of prospective drug candidates.

## Code availability

Code was implemented in the proprietary codebase, Diania, of the Odyssey Therapeutics generative drug discovery platform

## Contributions

Dr. Esben Jannik Bjerrum made the ideation of the approach, implementation of the prototype and production code changed on Diania, performed, and analyzed the similarity and docking tasks and wrote the draft of the paper as well as having overall supervision of the project. Raquel Lopez-Rios de Castro ported the augmented Hill-Climb code modifications to Diania, developed the DRD2 QSAR model and performed and analyzed the QSAR task and comparison of the AHC algorithm variants. Dr. Christian Margreitter and Dr. Thomas Blaschke provided help with the setup of the reinvent algorithm and scoring functions and provided helpful discussions and feedback on results. All authors read, edited, and approved the final paper

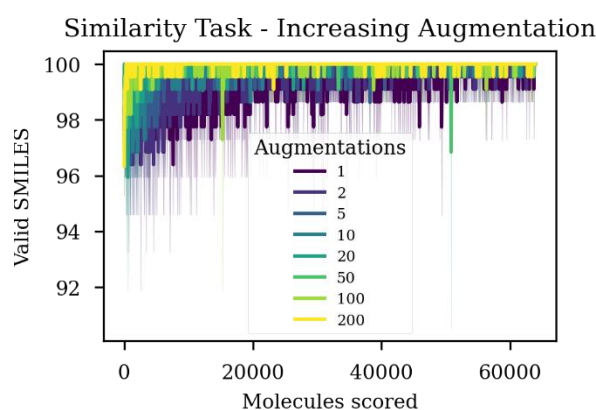
## References

- [1] E. J. Bjerrum and R. Threlfall, "Molecular Generation with Recurrent Neural Networks (RNNs)." May 2017. [Online]. Available: <http://arxiv.org/abs/1705.04612>
- [2] M. Olivecrona, T. Blaschke, O. Engkvist, and H. Chen, "Molecular de-novo design through deep reinforcement learning," *J. Cheminformatics*, vol. 9, no. 1, p. 48, Sep. 2017, doi: 10.1186/s13321-017-0235-x.
- [3] M. H. S. Segler, T. Kogej, C. Tyrchan, and M. P. Waller, "Generating focused molecule libraries for drug discovery with recurrent neural networks," *ACS Cent. Sci.*, vol. 4, no. 1, pp. 120–131, Jan. 2018, doi: 10.1021/acscentsci.7b00512.
- [4] A. Kadurin, S. Nikolenko, K. Khrabrov, A. Aliper, and A. Zhavoronkov, "DruGAN: An Advanced Generative Adversarial Autoencoder Model for de Novo Generation of New Molecules with Desired Molecular Properties in Silico," *Mol. Pharm.*, vol. 14, no. 9, pp. 3098–3104, Sep. 2017, doi: 10.1021/acs.molpharmaceut.7b00346.
- [5] R. Gómez-Bombarelli *et al.*, "Automatic Chemical Design Using a Data-Driven Continuous Representation of Molecules," *ACS Cent. Sci.*, vol. 4, no. 2, pp. 268–276, Feb. 2018, doi: 10.1021/acscentsci.7b00572.
- [6] T. Blaschke *et al.*, "REINVENT 2.0: An AI Tool for De Novo Drug Design," *J. Chem. Inf. Model.*, vol. 60, no. 12, pp. 5918–5922, Dec. 2020, doi: 10.1021/acs.jcim.0c00915.
- [7] J. Guo *et al.*, "Link-INVENT: Generative Linker Design with Reinforcement Learning." Apr. 25, 2022. doi: 10.26434/chemrxiv-2022-qkx9f.
- [8] V. Fialková *et al.*, "LibINVENT: Reaction-based Generative Scaffold Decoration for in Silico Library Design," *J. Chem. Inf. Model.*, p. acs.jcim.1c00469, Aug. 2021, doi: 10.1021/acs.jcim.1c00469.

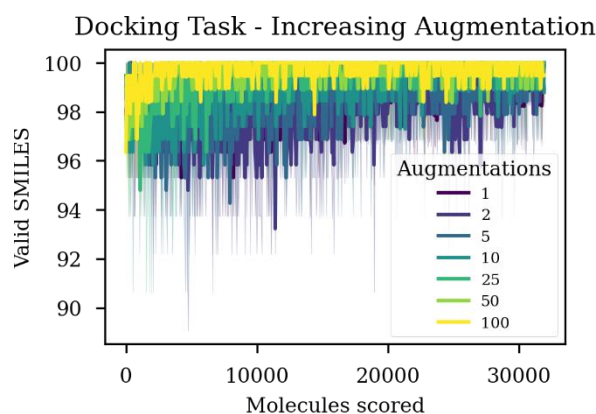
- [9] D. C. Elton, Z. Boukouvalas, M. D. Fuge, and P. W. Chung, "Deep learning for molecular design - A review of the state of the art," *Mol. Syst. Des. Eng.*, vol. 4, no. 4, pp. 828–849, 2019, doi: 10.1039/c9me00039a.
- [10] Y. Xu *et al.*, "Deep learning for molecular generation," *Future Med. Chem.*, p. fmc-2018-0358, Jan. 2019, doi: 10.4155/fmc-2018-0358.
- [11] M. Wang *et al.*, "Deep learning approaches for de novo drug design: An overview," *Curr. Opin. Struct. Biol.*, vol. 72, pp. 135–144, Feb. 2022, doi: 10.1016/j.sbi.2021.10.001.
- [12] M. Thomas, N. M. O'Boyle, A. Bender, and C. de Graaf, "Augmented Hill-Climb increases reinforcement learning efficiency for language-based de novo molecule generation." Apr. 15, 2022. doi: 10.26434/chemrxiv-2022-prz2r.
- [13] E. J. Bjerrum, "SMILES Enumeration as Data Augmentation for Neural Network Modeling of Molecules." arXiv, May 17, 2017. doi: 10.48550/arXiv.1703.07076.
- [14] J. Arús-Pous *et al.*, "Randomized SMILES strings improve the quality of molecular generative models," *J. Cheminformatics*, vol. 11, no. 1, pp. 1–13, 2019.
- [15] D. Neil *et al.*, "Exploring deep recurrent models with reinforcement learning for molecule design," *6th Int. Conf. Learn. Represent. ICLR 2018 - Workshop Track Proc.*, pp. 1–15, 2018.
- [16] N. Brown, M. Fiscato, M. H. S. Segler, and A. C. Vaucher, "GuacaMol: Benchmarking Models for de Novo Molecular Design," *J. Chem. Inf. Model.*, vol. 59, no. 3, pp. 1096–1108, Mar. 2019, doi: 10.1021/acs.jcim.8b00839.
- [17] W. Gao, T. Fu, J. Sun, and C. W. Coley, "Sample Efficiency Matters: A Benchmark for Practical Molecular Optimization." arXiv, Jun. 22, 2022. doi: 10.48550/arXiv.2206.12411.
- [18] P. Renz, D. Van Rompaey, J. K. Wegner, S. Hochreiter, and G. Klambauer, "On failure modes in molecule generation and optimization," *Drug Discov. Today Technol.*, vol. 32–33, pp. 55–63, 2019, doi: 10.1016/j.ddtec.2020.09.003.
- [19] P.-C. Kotsias, J. Arús-Pous, H. Chen, O. Engkvist, C. Tyrchan, and E. J. Bjerrum, "Direct steering of de novo molecular generation with descriptor conditional recurrent neural networks," *Nat. Mach. Intell.*, vol. 2, no. 5, pp. 254–265, 2020.
- [20] E. J. Bjerrum and B. Sattarov, "Improving chemical autoencoder latent space and molecular de novo generation diversity with heteroencoders," *Biomolecules*, vol. 8, no. 4, p. 131, 2018.
- [21] R. Irwin, S. Dimitriadis, J. He, and E. J. Bjerrum, "Chemformer: a pre-trained transformer for computational chemistry," *Mach. Learn. Sci. Technol.*, vol. 3, no. 1, p. 015022, Jan. 2022, doi: 10.1088/2632-2153/ac3ffb.
- [22] D. Sumner, J. He, A. Thakkar, O. Engkvist, and E. J. Bjerrum, "Levenshtein Augmentation Improves Performance of SMILES Based Deep-Learning Synthesis Prediction." 2020. doi: 10.26434/chemrxiv.12562121.v1.
- [23] T. Blaschke, O. Engkvist, J. Bajorath, and H. Chen, "Memory-assisted reinforcement learning for diverse molecular de novo design," *J. Cheminformatics*, vol. 12, no. 1, pp. 1–17, 2020, doi: 10.1186/s13321-020-00473-0.
- [24] "ReinventCommunity (jupyter notebook tutorials for REINVENT 3.2)." AstraZeneca - Molecular AI, <https://github.com/MolecularAI/ReinventCommunity>, Sep. 08, 2022. Accessed: Sep. 09, 2022. [Online]. Available: <https://github.com/MolecularAI/ReinventCommunity>
- [25] J. Guo *et al.*, "DockStream: a docking wrapper to enhance de novo molecular design," *J. Cheminformatics*, vol. 13, no. 1, p. 89, Nov. 2021, doi: 10.1186/s13321-021-00563-7.
- [26] R. A. Friesner *et al.*, "Glide: A New Approach for Rapid, Accurate Docking and Scoring. 1. Method and Assessment of Docking Accuracy," *J. Med. Chem.*, vol. 47, no. 7, pp. 1739–1749, Mar. 2004, doi: 10.1021/jm0306430.

- [27] S. Wang, T. Che, A. Levit, B. K. Shoichet, D. Wacker, and B. L. Roth, "Structure of the D2 dopamine receptor bound to the atypical antipsychotic drug risperidone," *Nature*, vol. 555, no. 7695, pp. 269–273, Mar. 2018, doi: 10.1038/nature25758.
- [28] H. M. Berman *et al.*, "The Protein Data Bank," *Nucleic Acids Res.*, vol. 28, no. 1, pp. 235–242, Jan. 2000, doi: 10.1093/nar/28.1.235.
- [29] D. Polykovskiy *et al.*, "Molecular Sets (MOSES): A Benchmarking Platform for Molecular Generation Models," *Front. Pharmacol.*, vol. 11, 2020, Accessed: Aug. 25, 2022. [Online]. Available: <https://www.frontiersin.org/articles/10.3389/fphar.2020.565644>
- [30] J. Sun *et al.*, "ExCAPE - DB : an integrated large scale dataset facilitating Big Data analysis in chemogenomics," *J. Cheminformatics*, pp. 1–9, 2017, doi: 10.1186/s13321-017-0203-5.
- [31] S. Margreitter, "ChemCharts." Sep. 07, 2022. Accessed: Sep. 09, 2022. [Online]. Available: <https://github.com/SMargreitter/ChemCharts>
- [32] L. McInnes, J. Healy, and J. Melville, "UMAP: Uniform Manifold Approximation and Projection for Dimension Reduction." arXiv, Sep. 17, 2020. doi: 10.48550/arXiv.1802.03426.
- [33] F. Pedregosa *et al.*, "Scikit-learn: Machine Learning in Python," *J. Mach. Learn. Res.*, vol. 12, no. null, pp. 2825–2830, Nov. 2011.
- [34] "RDKit: Open source cheminformatics." [Online]. Available: <http://www.rdkit.org>
- [35] J. Jumper *et al.*, "Highly accurate protein structure prediction with AlphaFold," *Nature*, vol. 596, no. 7873, Art. no. 7873, Aug. 2021, doi: 10.1038/s41586-021-03819-2.
- [36] F. Wong *et al.*, "Benchmarking AlphaFold-enabled molecular docking predictions for antibiotic discovery," *Mol. Syst. Biol.*, vol. 18, no. 9, p. e11081, Sep. 2022, doi: 10.15252/msb.202211081.
- [37] K. Papadopoulos, K. A. Giblin, J. P. Janet, A. Patronov, and O. Engkvist, "De novo design with deep generative models based on 3D similarity scoring," *Bioorg. Med. Chem.*, vol. 44, p. 116308, Aug. 2021, doi: 10.1016/j.bmc.2021.116308.

# Supplementary Material for “Faster and more diverse de novo molecular generation with double-loop reinforcement learning optimization using augmented SMILES”



Supplementary Figure 1 Valid SMILES for similarity task with increasing augmentations. All generations are in the high nineties but appears to be slightly higher with a higher number of augmentations.



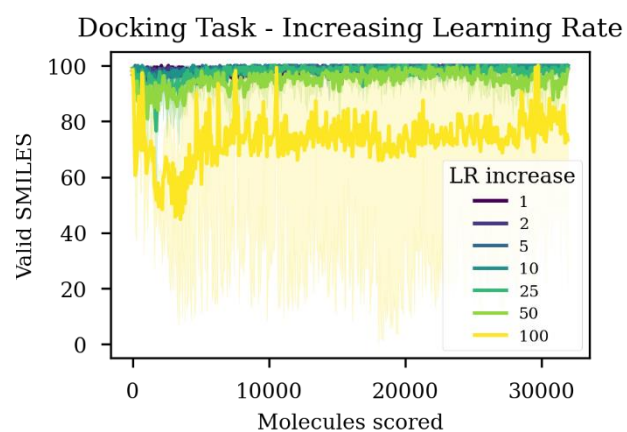
Supplementary Figure 2 Percentage valid SMILES per batch for the docking task with increases in augmentation. All runs are in the high nineties

Supplementary Table 1: Similarity task grid-search. Solved is when the exact target is obtained. Mean of solved is only including the runs that were solved, whereas mean is of all runs. The number of > characters denote how many runs were not solved. i.e. >> means two runs out of three weren't solved). Bold marks lowest numbers per column or both the augmentation scan and the learning rate scan.

		Similarit	Similarity	Similarity	Similarity >0.8	Solved	Solved

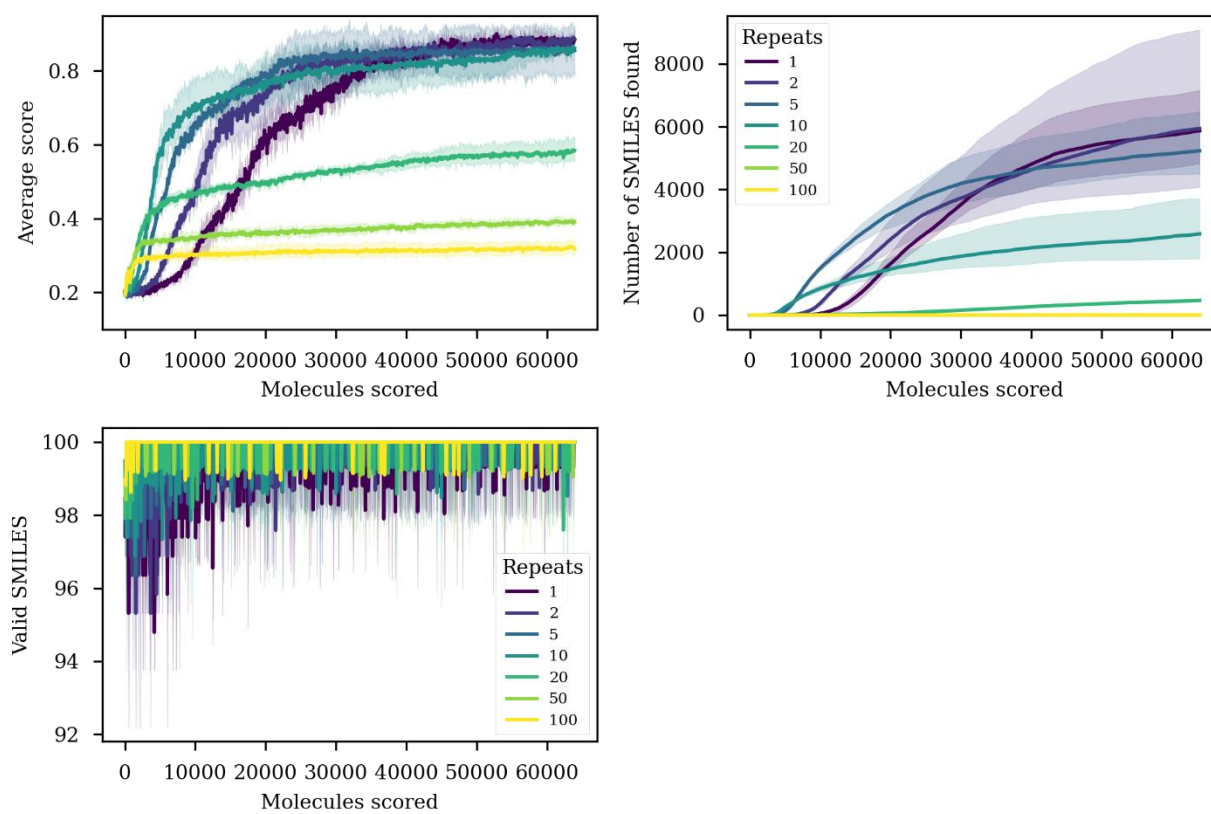
		y >0.5	>0.5	>0.8			
		Mean	Mean of Solved	Mean	Mean of Solved	Mean	Mean of Solved
x lr	x aug						
1	1	398.3	398.3	>>>500.0	NAN	301.3	301.3
1	2	258.3	258.3	>>>500.0	NAN	304	304
1	3	179.7	179.7	385.3	385.3	186.7	186.7
1	5	129	129	287.7	287.7	183.7	183.7
1	10	97	97	282.3	282.3	>494.7	242
1	20	64.3	64.3	184.7	184.7	>>760.7	282
2	1	258.7	258.7	>>>500.0	NAN	405.7	405.7
2	2	155.3	155.3	>443.7	415.5	>469.7	204.5
2	3	139.7	139.7	271	271	>428.0	142
2	5	93	93	279.7	279.7	>425.0	137.5
2	10	62.7	62.7	149.7	149.7	>378.7	68
2	20	47.7	47.7	169	169	>406.3	109.5
3	1	210	210	440.7	440.7	216.3	216.3
3	2	122.3	122.3	217.7	217.7	<b>122</b>	122
3	3	97.7	97.7	241.3	241.3	>425.0	137.5
3	5	75.7	75.7	288	288	>452.3	178.5
3	10	60.7	60.7	163.7	163.7	>>694.0	82
3	20	41.3	41.3	146.7	146.7	>>682.7	48
5	1	143.3	143.3	>417.3	376	>524.3	286.5
5	2	102.7	102.7	326.3	326.3	>>744.3	233
5	3	78	78	287.7	287.7	>>750.3	251
5	5	65	65	186.3	186.3	>>703.3	110
5	10	49.7	49.7	178	178	>>>1000.0	NAN
5	20	<b>35.7</b>	<b>35.7</b>	197.3	197.3	>>>1000.0	NAN
7	1	123	123	401.3	401.3	287.7	287.7
7	2	86	86	289	289	>>>1000.0	NAN
7	3	72.3	72.3	249.7	249.7	>>761.0	283

7	5	61.7	61.7	172.3	172.3	>>681.3	<b>44</b>
7	10	38.3	38.3	<b>106.7</b>	<b>106.7</b>	>367.3	51
7	20	38.3	38.3	184.7	184.7	>>684.3	53
15	1	99.3	99.3	366.7	366.7	>>797.3	392
15	2	66.7	66.7	212.3	212.3	>>715.3	146
15	3	50.7	50.7	216	216	>>>1000. 0	NAN
15	5	44	44	>272.3	158.5	>>>1000. 0	NAN
15	10	49.7	49.7	144.3	144.3	>>685.3	56
15	20	59.7	59.7	251.7	251.7	>>>1000. 0	NAN



Supplementary Figure 3 Effect on increasing learning rate on SMILES validity. Highest learning rates lead to instability in generation and lower validity.

## Similarity Task - Repeats of Sampled



Supplementary Figure 4: Effects of using the same sequences many times in the inner loop.